

# Evidence for Seed-Mediated Nucleation in the Chemical Reduction of Gold Salts to Gold Nanoparticles

Nikhil R. Jana,\* Latha Gearheart, and Catherine J. Murphy\*

Department of Chemistry and Biochemistry, Graduate Science Research Center,  
University of South Carolina, Columbia, South Carolina 29208

Received August 17, 2000. Revised Manuscript Received May 5, 2001

Central to the concept of seed-mediated growth of nanoparticles is that small nanoparticle seeds serve as nucleation centers to grow nanoparticles to a desired size. We have examined this common assumption in a model system, the wet chemical synthesis of gold nanoparticles via reduction of a gold salt, by transmission electron microscopy and electronic absorption spectroscopy. We find that changing the seed concentration does affect the size of the product nanoparticles, but the method of reagent addition drastically affects the outcome even more. For fast addition of reducing agent, the presence of seeds appears to promote the formation of more seeds instead of growth. The observed nucleations are drastically enhanced (99%) compared to particle growth. For slow addition of reducing agent, the seeds do grow, but the product nanoparticle's degree of homogeneity in shape is compromised. For higher concentrations of seeds, nanoparticle growth is better controlled for slow addition of reducing agent compared to fast addition of reducing agent. We propose a mechanistic step to explain the commonly observed size distribution.

## Introduction

Metal nanoparticles are of great current interest due to their functions as chemical catalysts, adsorbents, biological stains, and elements of novel nanometer-scale optical, electronic, and magnetic devices.<sup>1–13</sup> As the size of the particle decreases to the 1–100 nm range, it is well-known that the electronic, optical, catalytic, and thermodynamic properties of metal particles deviate from bulk properties.<sup>2,3,9–11</sup> Size effects are also observed in surface-enhanced Raman scattering (SERS) experiments, where gold and silver nanoparticles are frequently used as substrates for signal enhancements.<sup>14–16</sup>

Much work has been devoted to the synthesis of metal nanoparticles, especially the relatively easy solution-phase chemical reduction methods.<sup>17</sup> There is still a significant challenge, however, in understanding and predicting nanoparticle size and shape from a given set of synthetic conditions.<sup>18–21</sup> The use of ligand stabilizers, including dendrimers, is one key element that allows for a degree of control in nanoparticle synthesis.<sup>4,5,17,22–24</sup> The general mechanistic steps frequently assumed, but less often measured, in nanoparticle synthesis are nucleation and growth stages;<sup>5,9,10,25–29</sup> ideally, nucleation and growth would be separated in time to achieve

\* To whom correspondence should be addressed. E-mail: (N.R.J.) jana@mail.chem.sc.edu, (C.J.M.) murphy@mail.chem.sc.edu.

(1) Thomas, J. M. *Pure Appl. Chem.* **1988**, *60*, 1517.  
(2) Lewis, N. S. *Chem. Rev.* **1993**, *93*, 2693.  
(3) Schmid, G. *Cluster and Colloids: from Theory to Applications*; VCH: New York, 1994.  
(4) Schmid, G.; Baumle, M.; Geerkens, M.; Helm, I.; Osemann, C.; Sawitowski, T. *Chem. Soc. Rev.* **1999**, *28*, 179.  
(5) Aiken, J. D.; Finke, R. G. *J. Mol. Catal., A* **1999**, *145*, 1.  
(6) Rao, C. N. R.; Kulkarni, G. U.; Thomas, P. J.; Edwards, P. P. *Chem. Soc. Rev.* **2000**, *29*, 27.  
(7) Templeton, A. C.; Wuelfing, M. P.; Murray, R. W. *Acc. Chem. Res.* **2000**, *33*, 27.  
(8) Henglein, A. *Chem. Rev.* **1989**, *89*, 1861.  
(9) Henglein, A. *J. Phys. Chem.* **1993**, *97*, 5457.  
(10) Belloni, J. *Curr. Opin. Colloid Interface Sci.* **1996**, *1*, 184.  
(11) Chen, S. W.; Ingram, R. S.; Hostetler, M. J.; Pietron, J. J.; Murray, R. W.; Schaaff, T. G.; Khoury, J. T.; Alvarez, M. M.; Whetten, R. L. *Science* **1998**, *280*, 2098.  
(12) Jana, N. R.; Sau, T. K.; Pal, T. *J. Phys. Chem. B* **1999**, *103*, 115.  
(13) Freund, P. L.; Spiro, M. *J. Phys. Chem.* **1985**, *89*, 1074.  
(14) Nie, S.; Emory, S. R. *Science* **1997**, *275*, 1102.  
(15) Krug, J. T.; Wang, G. D.; Emory, S. R.; Nie, S. M. *J. Am. Chem. Soc.* **1999**, *121*, 9208.  
(16) Kneipp, K.; Kneipp, H.; Manoharan, R.; Hanlon, E. B.; Itzkan, I.; Dasari, R. R.; Feld, M. S. *Appl. Spectrosc.* **1998**, *52*, 1493.

(17) (a) Brust, M.; Walker, M.; Bethell, D.; Schiffrin, D.; Whyman, R. *J. Chem. Soc., Chem. Commun.* **1994**, 801. (b) Bonnemann, H.; Braun, G.; Brijoux, W.; Brinkmann, R.; Tilling, A. S.; Seevogel, K.; Siepen, K. *J. Organomet. Chem.* **1996**, *520*, 143. (c) Hostetler, M. J.; Wingate, J. E.; Zhong, C. J.; Harris, J. E.; Vachet, R. W.; Clark, M. R.; Londono, J. D.; Green, S. J.; Stokes, J. J.; Wignall, G. D.; Glish, G. L.; Porter, M. D.; Evans, N. D.; Murray, R. W. *Langmuir* **1998**, *14*, 17. (d) Brown, K. R.; Walter, D. G.; Natan, M. J. *Chem. Mater.* **2000**, *12*, 306. (e) Weare, W. W.; Reed, S. M.; Warner, M. G.; Hutchison, J. E. *J. Am. Chem. Soc.* **2000**, *122*, 12890.  
(18) Adair, J. H.; Suvaci, E. *Curr. Opin. Colloid Interface Sci.* **2000**, *5*, 160.  
(19) Peng, X.; Wickham, J.; Alivisatos, A. P. *J. Am. Chem. Soc.* **1998**, *120*, 5343.  
(20) Ahmadi, T.; Wang, Z. L.; Green, T. C.; Henglein, A.; El-Sayed, M. A. *Science* **1996**, *272*, 1924.  
(21) Bradley, J. S.; Tesche, B.; Busser, W.; Maase, M.; Reetz, M. T. *J. Am. Chem. Soc.* **2000**, *122*, 4631.  
(22) He, J. A.; Valluzzi, R.; Yang, K.; Dolukhanyan, T.; Sung, C. M.; Kumar, J.; Tripathy, S. K.; Samuelson, L.; Balogh, L.; Tomalia, D. A. *Chem. Mater.* **1999**, *11*, 3268.  
(23) Chechik, V.; Crooks, R. M. *Langmuir* **1999**, *15*, 6364.  
(24) Esumi, K.; Suzuki, A.; Yamahira, A.; Torigoe, K. *Langmuir* **2000**, *16*, 2604.  
(25) Goia, D. V.; Matijevic, E. *New J. Chem.* **1998**, *22*, 1203.  
(26) Watzky, M. A.; Finke, R. G. *J. Am. Chem. Soc.* **1997**, *119*, 10382.  
(27) Belloni, J. *Radiat. Res.* **1998**, *150*, S9.  
(28) Belloni, J.; Mostafavi, M.; Remita, H.; Marignier, J. L.; Delcourt, M. O. *New J. Chem.* **1998**, *22*, 1239.

a narrow size distribution (and possible shape distribution) of the product nanoparticles.

For the reduction of metal salts to metallic nanoparticles, the metal atoms and clusters formed at the early stages of the reaction have short lifetimes and are extremely reactive.<sup>8–10,27–29</sup> Belloni et al. and Henglein et al. have established that the redox potentials of coordination compounds containing single metal ions are very negative, and with increasing cluster nuclearity they approach their bulk electrode values.<sup>8–10,30–36</sup> Due to this size-dependent redox property, often the chemical reduction of a metal salt is very dependent on solution conditions and even the nature of the reaction vessel.<sup>10,37</sup> This may be the reason that induction periods and autocatalytic reduction kinetics in metal salt reduction are observed.<sup>37–43</sup>

The use of preformed metallic seeds as nucleation centers in nanoparticle synthesis has a long history.<sup>17d,39,44–53</sup> However, many of the methods to prepare metallic colloidal particles of uniform size from the growth of metallic seeds are not as successful as they could be due to further nucleation during the “growth” part of the reaction.<sup>53–55</sup> By examination of the kinetics of a reaction, Finke has evidence for a continuous low level of nucleation followed by fast autocatalytic growth that contributes to the observed narrow size distribution of metal clusters,<sup>26</sup> while others have transmission electron microscopy (TEM) evidence for the appearance of small particles and hence a broadening of the particle size distribution during the intermediate period of particle formation.<sup>56,57</sup> Here, we study the effect of 12 nm gold seed concentration in the solution-phase prepara-

tion of gold nanoparticles for a range of reducing agents and conditions. We observe that the presence of seeds appears to cause additional nucleation. Thus, the improved monodispersity that should be achieved by separating the nucleation and growth steps in time is not guaranteed by the presence of seeds. Other parameters we vary in our experiments are the rate of addition of reducing agent to the metal seed and metal salt solution and the chemical identity of the reducing agent. By controlling the conditions, we are able to prepare spherical gold nanoparticles 20–100 nm in diameter that have relatively narrow size distributions (less than  $\pm 20\%$  relative standard deviation). Insight into the mechanism of nanoparticle formation is gained from this study.

## Experimental Section

**Materials.** Sodium citrate (Fisher),  $\text{HAuCl}_4 \cdot 3\text{H}_2\text{O}$  (Sigma), ascorbic acid (Aldrich), hydrazine dihydrochloride (Aldrich),  $\text{NaBH}_4$  (Mallinckrodt), sodium dodecyl sulfate (Sigma), and  $\text{AgNO}_3$  (Aldrich) were used as received. Ultrapure deionized water (Continental Water Systems) was used for all solution preparations and experiments.

**Instrumentation.** Particle sizing studies of the gold nanoparticles were performed using a JEOL JEM-100CXII transmission electron microscope operating at 100 kV. Sizing was enabled using an AMT Kodak Megaplug digital camera and software. Samples were prepared for electron microscopy by evaporating 2  $\mu\text{L}$  of nanoparticle solution (at 25 °C) on Formvar-coated copper grids. To understand the overall character of the nanoparticles, we explored the entire grid at varying magnifications. Approximately 100 nanoparticles from each sample were measured for size distribution. Electronic absorption spectra of nanoparticle solutions were collected with a CARY 500 scan UV–vis–near-IR spectrophotometer.

**Preparation of 12 nm Gold Seeds.** Solutions of citrate-reduced gold nanoparticles were prepared according to the Frens method.<sup>58</sup> All glassware was rigorously cleaned in aqua regia solution before use. A 100 mL sample of aqueous  $\text{HAuCl}_4 \cdot 3\text{H}_2\text{O}$  ( $2.5 \times 10^{-4}$  M) was prepared in a 250 mL conical flask. The solution was brought to a boil while stirring, and 3 mL of 1% aqueous sodium citrate was added. The solution underwent a series of color changes before finally turning wine red. The boiling and stirring was continued for 30 min after the final color change. After cooling to room temperature, the gold nanoparticle solution was diluted to 100 mL using deionized water to replace the water evaporated during boiling. The gold solutions consisted of mostly isolated, almost spherical, particles with a mean diameter of  $12 \pm 2$  nm according to TEM.

**Preparation of Gold Nanoparticles in the Presence of Seed.** Solutions of differently sized gold nanoparticles were prepared using three different methods (i–iii) described below.

(i) *Preparation of Gold Particles in the Presence of 12 nm Seed by Fast Addition of Reducing Agent.* Six sets of solutions (A–F) were prepared in the presence of varying amounts of 12 nm seed (15.0–0.0 mL) according to Table 1. Enough aqueous  $\text{HAuCl}_4 \cdot 3\text{H}_2\text{O}$  was added to each seed solution so that the final gold atom concentration including gold salt and gold seed became  $1.0 \times 10^{-4}$  M Au after the final dilution. While the solution was stirring, 4 mL of ascorbic acid ( $1.0 \times 10^{-2}$  M) was added all at once at room temperature. After the ascorbic acid was added, the solution's color changed, and the final color varied from red to rust depending on the amount of seed added. Each gold solution was diluted up to 250 mL with deionized water.

(56) Seshadri, R.; Subbanna, G. N.; Vijayakrishnan, V.; Kuklarni, G. U.; Anathakrishna, G.; Rao, C. N. R. *J. Phys. Chem.* **1995**, *99*, 5639.

(57) Chow, M. K.; Zukoski, C. F. *J. Colloid Interface Sci.* **1994**, *165*, 97.

(58) Frens, G. *Nature* **1973**, *241*, 20.

(29) Gachard, E.; Remita, H.; Khatouri, J.; Keita, B.; Nadjio, L.; Belloni, J. *New J. Chem.* **1998**, *22*, 1257.

(30) Delcourt, M. O.; Belloni, J. *Radiochem. Radioanal. Lett.* **1973**, *13*, 329.

(31) Henglein, A. *Ber. Bunsen-Ges. Phys. Chem.* **1977**, *81*, 556.

(32) Mosseri, S.; Henglein, A.; Janata, E. *J. Phys. Chem.* **1989**, *93*, 6791.

(33) Henglein, A.; Janata, E.; Fojtik, A. *J. Phys. Chem.* **1992**, *96*, 4734.

(34) Remita, S.; Archirel, P. and Mostafavi, M. *J. Phys. Chem.* **1995**, *99*, 13198.

(35) Texier, I.; Remita, S.; Archirel, P.; Mostafavi, M. *J. Phys. Chem.* **1996**, *100*, 12472.

(36) Cointet, C. de; Mostafavi, M.; Khatouri, J.; Belloni, J. *J. Phys. Chem. B* **1997**, *101*, 3512.

(37) Quinn, M.; Mills, G. *J. Phys. Chem.* **1994**, *98*, 9840.

(38) Belloni, J.; Mostafavi, M.; Marignier, J. L.; Amblard, J. J. *Imaging Sci. Technol.* **1991**, *35*, 68.

(39) Turkevich, J.; Stevenson, P. C.; Hillier, J. *Faraday Discuss. Chem. Soc.* **1951**, *11*, 55.

(40) Huang, Z. Y.; Mills, G.; Hajek, B. *J. Phys. Chem.* **1993**, *97*, 11542.

(41) Pal, T.; Sau, T. K.; Jana, N. R. *Langmuir* **1997**, *13*, 1481.

(42) Han, M. Y.; Quek, C. H.; Huang, W.; Chew, C. H.; Gan, L. M. *Chem. Mater.* **1999**, *11*, 1144.

(43) Rodríguez-Sánchez, L.; Blanco, M. C.; López-Quintela, M. A. *J. Phys. Chem. B* **2000**, *104*, 9683.

(44) Zsigmondy, R.; Thiesen, P. A. *Das Kolloide Gold*; Veragsges.: Leipzig, 1925.

(45) Schneider, S.; Halbig, P.; Grau, H.; Nickel, U. *Photochem. Photobiol.* **1994**, *60*, 605.

(46) Shirtcliffe, N.; Nickel, U.; Schneider, S. *J. Colloid Interface Sci.* **1999**, *211*, 122.

(47) Brown, K. R.; Natan, M. J. *Langmuir* **1998**, *14*, 726.

(48) Henglein, A.; Meisel, D. *Langmuir* **1998**, *14*, 7392.

(49) Henglein, A.; Giersig, M. *J. Phys. Chem. B* **1999**, *103*, 9533.

(50) Henglein, A. *J. Phys. Chem. B* **2000**, *104*, 1206.

(51) Teranishi, T.; Miyake, M. *Chem. Mater.* **1998**, *10*, 594.

(52) Teranishi, T.; Hosoe, M.; Tanaka, T.; Miyake, M. *J. Phys. Chem. B* **1999**, *103*, 3818.

(53) Watzky, M. A.; Finke, R. G. *Chem. Mater.* **1997**, *9*, 3083.

(54) Westgren, Z. *Anorg. Chem.* **1915**, *93*, 151.

(55) Wiesner, J.; Wokaun, A. *Chem. Phys. Lett.* **1989**, *157*, 569.

**Table 1. Preparing Differently Sized Gold Nanoparticles in the Presence of 12 nm Gold Seed<sup>a</sup>**

sample	vol of added seed (0.25 mM in Au), mL	vol of added HAuCl <sub>4</sub> (10 mM), mL	sample	vol of added seed (0.25 mM in Au), mL	vol of added HAuCl <sub>4</sub> (10 mM), mL
A, A'	15.0	2.12	D, D'	0.24	2.49
B, B'	2.25	2.44	E, E'	0.09	2.50
C, C'	0.79	2.48	F, F'	0	2.50

<sup>a</sup> Samples A–F were prepared by fast addition of reducing agent (method i); samples A'–F' were prepared by slow addition of reducing agent (method ii).

**Table 2. Preparing Differently Sized Gold Nanoparticles in the Presence of Gold Seed: Step-by-Step Method**

sample	vol of added seed (0.1 mM in Au), mL	vol of added HAuCl <sub>4</sub> (10 mM), mL	sample	vol of added seed (0.1 mM in Au), mL	vol of added HAuCl <sub>4</sub> (10 mM), mL
G	37.5 (A) (Table 1)	2.12	I	75 (H)	1.75
H	87.5 (G)	1.62	J	100 (I)	1.50

(ii) *Preparation of Gold Particles in the Presence of 12 nm Seed by Slow Addition of Reducing Agent.* Six sets of solutions (A'–F') were prepared by mixing different volumes of 12 nm seed with HAuCl<sub>4</sub>·3H<sub>2</sub>O as described above and in Table 1. Each solution was diluted up to 150 mL using deionized water. While the solution was stirring, 100 mL of freshly prepared dilute ascorbic acid ( $4 \times 10^{-4}$  M) was added slowly (10 mL/min) from a buret.

(iii) *Preparation of Gold Particles by Step by Step Seeding.* In this method, particles are prepared and then used as seeds for producing larger particles. The larger particles are then used as seeds for producing even larger particles, and so on. Table 2 shows the ratio of seed to HAuCl<sub>4</sub>·3H<sub>2</sub>O for sets G–J. For example, for set G, 37.5 mL from set A is used as seed and mixed with 2.12 mL of HAuCl<sub>4</sub>·3H<sub>2</sub>O (10 mM). Each solution was diluted up to 150 mL using deionized water. While the solution was stirring, 100 mL of freshly prepared dilute ascorbic acid ( $4 \times 10^{-4}$  M) was added slowly (10 mL/min) from a buret.

**Kinetics Study.** The kinetics of gold particle growth was studied by monitoring the change in the absorbance maximum of the gold particle plasmon band with time. The particle solutions were prepared by reducing Au<sup>3+</sup> with ascorbic acid both in the presence and in the absence of seed. Sodium dodecyl sulfate was added as a stabilizer to decrease the reduction rate to a time scale amenable to available instrumentation.<sup>12,41</sup>

## Results

**Influence of Seed Concentration on the Formation of Gold Nanoparticles: Fast Addition of Reducing Agent.** Under the acidic reaction conditions described here, virtually all of the gold salt is in the AuCl<sub>4</sub><sup>-</sup> form; no hydroxide–chloride complexes of Au<sup>3+</sup> are stable.<sup>59</sup> Preparation of the 12 nm seed itself requires high (~100 °C) temperatures and a weak reducing agent (citrate) according to the Frens method.<sup>58</sup> The use of a stronger reducing agent (borohydride) allows the preparation of seeds to be performed at room temperature (see below), but the nanoparticles tend to be more heterogeneous in size than the citrate-reduced nanoparticles.

Figure 1 shows the electronic absorption spectra of gold nanoparticles prepared by the reduction of HAuCl<sub>4</sub> with ascorbic acid in the presence of the 12 nm seeds; room temperature is sufficient for these reactions to proceed on a time scale commensurate with the seed preparation. The spectra correspond to the “fast addition of reducing agent” conditions described above (method i). The concentration of the seed decreases from A to E;

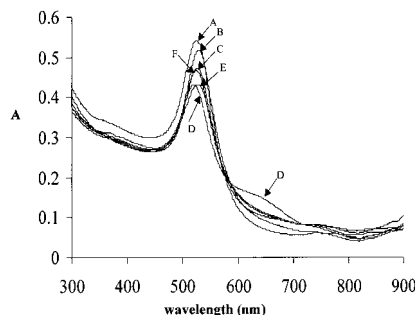


**Figure 1.** Extinction spectra of Au particles prepared by fast addition of reducing agent. The seed concentrations were decreased from A to E, and no seed was present for F (see Table 1 for experimental conditions).

F contains no seed. Solutions A, B, C, and F were stable for more than 1 week, but solutions D and E were stable for only a few hours. The shapes of the absorption spectra remain roughly constant, with a plasmon absorption band at ~530 nm. Sample D in addition shows a weak band at 600–700 nm, which is usually taken as an indication of either particle elongation or aggregation.<sup>60,61</sup> In the present case the origin of the weak band is due to the presence of large and small particles and a partial aggregation between them as seen in the TEM images (see below). We believe that aggregation also caused the lower stability of sets D and E. The magnitude of the plasmon absorption band of the nanoparticles prepared by method i varies with seed concentration: the lower absorbance for low amounts of seed (D and E) suggests a relatively greater population of small particles compared to those of A, B, and C. Other workers have noted size-dependent extinction coefficients of gold nanoparticles with decreasing size in the 2–10 nm range, with smaller particles producing lower extinction coefficients.<sup>60,62</sup> For samples A and B, with the largest amount of seed, the absorbance is the largest, suggesting a greater population of larger particles compared to those of C, D, E, and F.

Figures 2 and 3 show the electron micrographs and histograms, respectively, of gold nanoparticles prepared by the reduction of gold salt with ascorbic acid added all at once in the presence of varying amounts of 12 nm gold seeds. Figure 3 also includes the data for the seed itself. When ascorbic acid is used to reduce gold salt at

(59) (a) Goia, D. V.; Matijevic, E. *Colloids Surf., A* **1999**, *146*, 139. (b) Privman, V.; Goia, D. V.; Park, J.; Matijevic, E. *J. Colloid Interface Sci.* **1999**, *213*, 36.

(60) Link S, El-Sayed, M. A. *J. Phys. Chem. B* **1999**, *103*, 8410. (61) Lazarides, A. A.; Schatz, G. C. *J. Phys. Chem. B* **2000**, *104*, 460. (62) Alvarez, M. M.; Khoury, J. T.; Schaaff, T. G.; Shafiqullin, M. N.; Vezmar, I.; Whetten, R. L. *J. Phys. Chem.* **1997**, *101*, 3706.



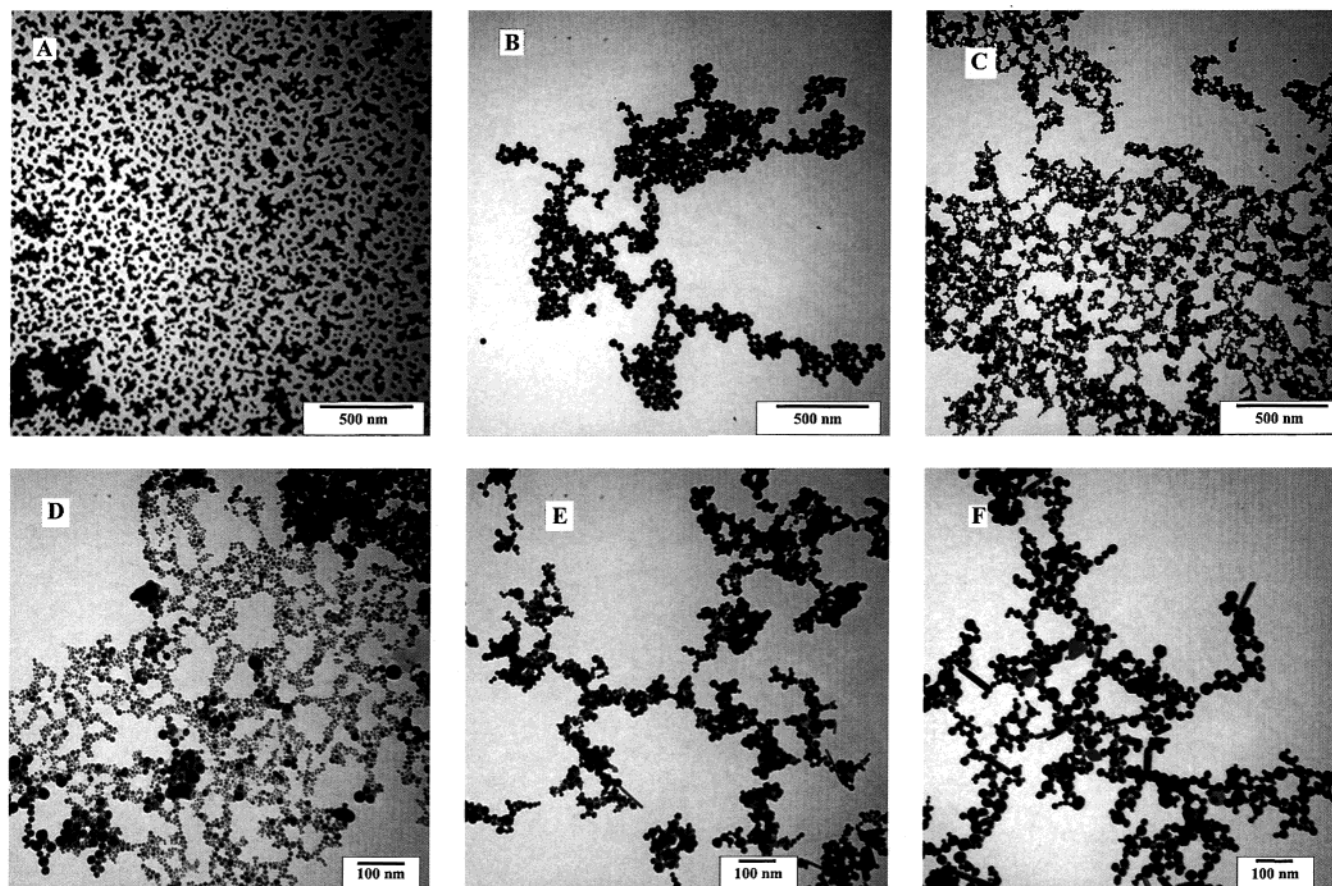


**Figure 2.** Representative electron micrographs of Au particles formed by fast addition of ascorbic acid corresponding to spectra A–F shown in Figure 1.

room temperature, in the absence of seed (F), many differently sized spherical particles are produced, including a number of rods. (The histograms only reflect the sizes of the spherical products.)

If growth alone occurs on the seed surface, then the average particle size should increase from sample A to sample E as the amount of seed is decreased. But this is not the case (Figures 2 and 3). In sample D the average particle diameter (10 nm) is even smaller than that of the seed (12 nm), and the histogram shows that most of the particles in D are less than 12 nm in diameter. Thus, the presence of seed under these conditions appears to give rise to more nucleation events. We estimated the concentration of seeds and nanoparticles produced by first knowing the total amount of Au atoms in solution for seed plus gold from the added salt and then determining how many atoms would fit in each particle. The volume of a sphere corresponding to the seed or the resultant particles (12 nm seed and ~20–48 nm particle) was calculated, and the total number of atoms fitting into each volume was determined using the crystal structure of gold (cubic unit cell 4.0786 Å on edge, 4 gold atoms/unit cell), giving us the average number of atoms per particle. The number of particles in each sample was calculated by dividing the total number of gold atoms by the atoms per particle. This was converted to the number of particles per liter by dividing by the sample volume. The results are summarized in Table 3. One caveat in this argument is that we are limited to what we can observe in the TEM images or infer from the UV–vis absorption spectra;

nanoparticles less than 1 nm in diameter are not observable by these means.

**Influence of Seed Concentration on the Formation of Gold Nanoparticles: Slow Addition of Reducing Agent or Step-by-Step Seeding.** It is possible that the sudden appearance of ascorbic acid in the seed/gold salt solutions above promotes the formation of more seeds instead of growth (see below for more details). If this is true, then the slow addition of more dilute concentrations of ascorbic acid should suppress further seed formation and promote growth. The slow addition of reducing agent (method ii) or the step-by-step seeding method (method iii), which incorporates slow addition of reducing agent, did give improved nanoparticle products in terms of monodispersity (less than  $\pm 20\%$  relative standard deviation) in product sphere size (Tables 3 and 4, Figures 4–6). Both methods ii and iii gave similar results; only the data for method ii will be discussed. Table 4 summarizes the results for the gold nanoparticles prepared according to method ii. Figures 4–6 show the UV–vis spectra, transmission electron micrographs, and histograms, respectively, for these particles. Figure 4S also includes the absorption spectrum of the seed solution. The concentrations of seed, gold salt, and reducing agent used to prepare the particles whose spectra are shown in Figure 4 are the same as those for Figure 1; the only difference is the manner in which the reducing agent was added. However, the UV–vis spectra are considerably different (Figures 1 and 4). For those particles in which the ascorbic acid was added slowly, the plasmon band

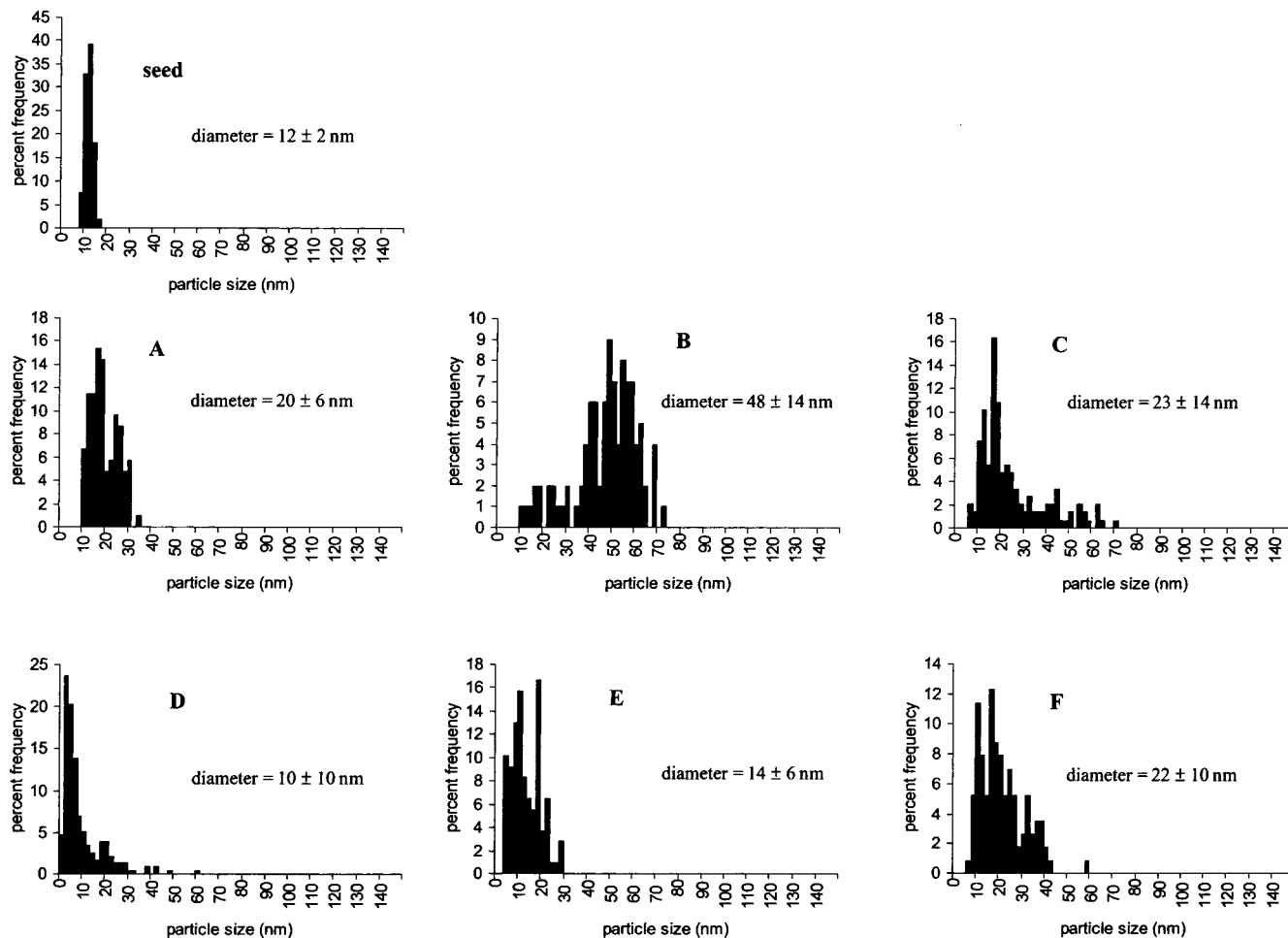


**Figure 3.** Size distribution histograms for Au seed and Au particles formed by fast addition of ascorbic acid corresponding to Figures 1 and 2.

**Table 3. Summary of Results for Gold Nanoparticles Prepared by Fast Addition of Reducing Agent (Method i)**

sample	seed concentration (no. of seeds/L) <sup>a</sup>	particle size and concn		addnl nucleation beyond seed (%) <sup>b</sup>
		diam (nm)	concn (no. of particles/L)	
A	$1.7 \times 10^{14}$	$20 \pm 6$	$2.4 \times 10^{14}$	~30
B	$2.5 \times 10^{13}$	$48 \pm 14$	$1.8 \times 10^{13}$	none
C	$8.9 \times 10^{12}$	$23 \pm 14$	$1.6 \times 10^{14}$	~94
D	$2.7 \times 10^{12}$	$10 \pm 10$	$1.9 \times 10^{15}$	~99
E	$1.0 \times 10^{12}$	$14 \pm 6$	$7.1 \times 10^{14}$	~99
F	0	$22 \pm 10$	$1.8 \times 10^{14}$	NA (no seed)

<sup>a</sup> Seed concentration is calculated by assuming all  $\text{Au}^{3+}$  is converted to  $\text{Au}^0$  seeds 12 nm in diameter as described in the text. <sup>b</sup> Additional nucleation =  $\{([\text{total particle}] - [\text{seed}])/[\text{total particle}]\} \times 100$ . NA = not applicable.

**Table 4. Summary of Results for Gold Nanoparticles Prepared by Slow Addition of Reducing Agent (Method ii)**

sample <sup>a</sup>	particle size and concn		concn (no. of particles/L)	additional nucleation beyond seed (%)
	measd diam (nm)	calcd diam <sup>b</sup> (nm)		
A'	$24 \pm 4$	23	$1.4 \times 10^{14}$	none
B'	$49 \pm 10$	43	$1.7 \times 10^{13}$	none
C'	$74 \pm 11$	60	$4.8 \times 10^{12}$	none
D'	$96 \pm 18$	90	$2.2 \times 10^{12}$	none

<sup>a</sup> Particles synthesized by method ii and with relatively large average diameters (samples E' and F') had irregular shapes. Since we assume the particles to be spheres in our calculations, these particles were not given consideration for subsequent columns in Table 4. <sup>b</sup> The calculated diameter was determined from the following equation:  $r = r_s \{ ([M_a] + [M_0])/[M_0] \}^{1/3}$ , where  $r_s$  and  $r$  indicate particle radii for seeds and larger particles respectively, and  $[M_0]$  and  $[M_a]$  indicate metal concentrations in seeds and added ion. This calculation assumes all seeds grow.

gradually red-shifts as the seed concentration decreases, indicating larger average particle diameters<sup>60</sup> as seed concentration decreases. This is confirmed by TEM (Figures 5 and 6), which shows that larger nanoparticles

on average were formed as the amount of seed decreased. We calculated how big the particles should be if all seeds grow and only growth occurs, and the calculated diameters and experimental diameter are

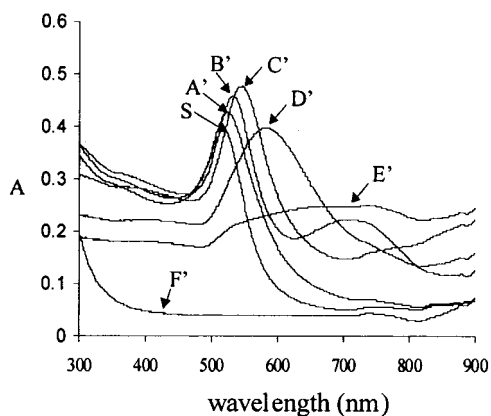


**Figure 4.** Extinction spectra of Au particles prepared by slow addition of reducing agent. The seed concentrations were decreased from A' to E', and no seed was present for F' (see Table 1 for experimental conditions). S represents the 12 nm seed prepared by citrate reduction.

similar (Table 4). No seed-sized (or smaller) particles are observed, suggesting that no additional nucleation events took place during the preparation of the nanoparticles when the reducing agent was added sufficiently slowly. In the absence of seed (F'), the reaction vessel became coated with a purple film, indicating extensive reduction at the vessel surface, and only a few nanoparticles remained in solution as indicated from the absorption spectrum (Figure 4F'). The TEM image of solution F' (not shown) shows few particles which are aggregates of large and small particles. In the TEM images of B', C', D', and E' there are a number of

platelet and rodlike nanoparticles as well (with an additional long-wavelength plasmon band corresponding to those shapes<sup>60</sup>), which poses complications for morphological control of nanoparticles. We have examined the use of additives in the reaction mixture to suppress nonspherical particle products (see below).

**Influence of the Chemical Nature of the Reducing Agent on the Formation of Gold Nanoparticles from Seeds.** To understand whether seed-promoted nucleation for fast addition of reducing agent was a phenomenon peculiar to ascorbic acid, or was applicable to other reducing agents, we compared the performance of ascorbic acid to that of sodium borohydride, hydrazine, and sodium citrate for making gold nanoparticles in the presence of seeds. We chose the conditions of method i, set D (which gave many particles smaller than the original seeds). The transmission electron micrographs of the gold nanoparticles prepared with these other reducing agents show that other (weak) reducing agents do produce nucleation events in addition to/instead of growth, as judged by the appearance of nanoparticles smaller than the starting seeds in the TEM images (Figure 1 in the Supporting Information). However, there are some differences between the reducing agents. Citrate reduction of gold salt in the presence of 12 nm gold seeds produces a partial precipitate, and the 2–10 nm nanoparticles that were in solution were extensively aggregated. We found that small gold nanoparticles prepared via the fast addition of hydrazine in the presence of 12 nm seeds were unstable, and accordingly we added sodium dodecyl sulfate (SDS) as a

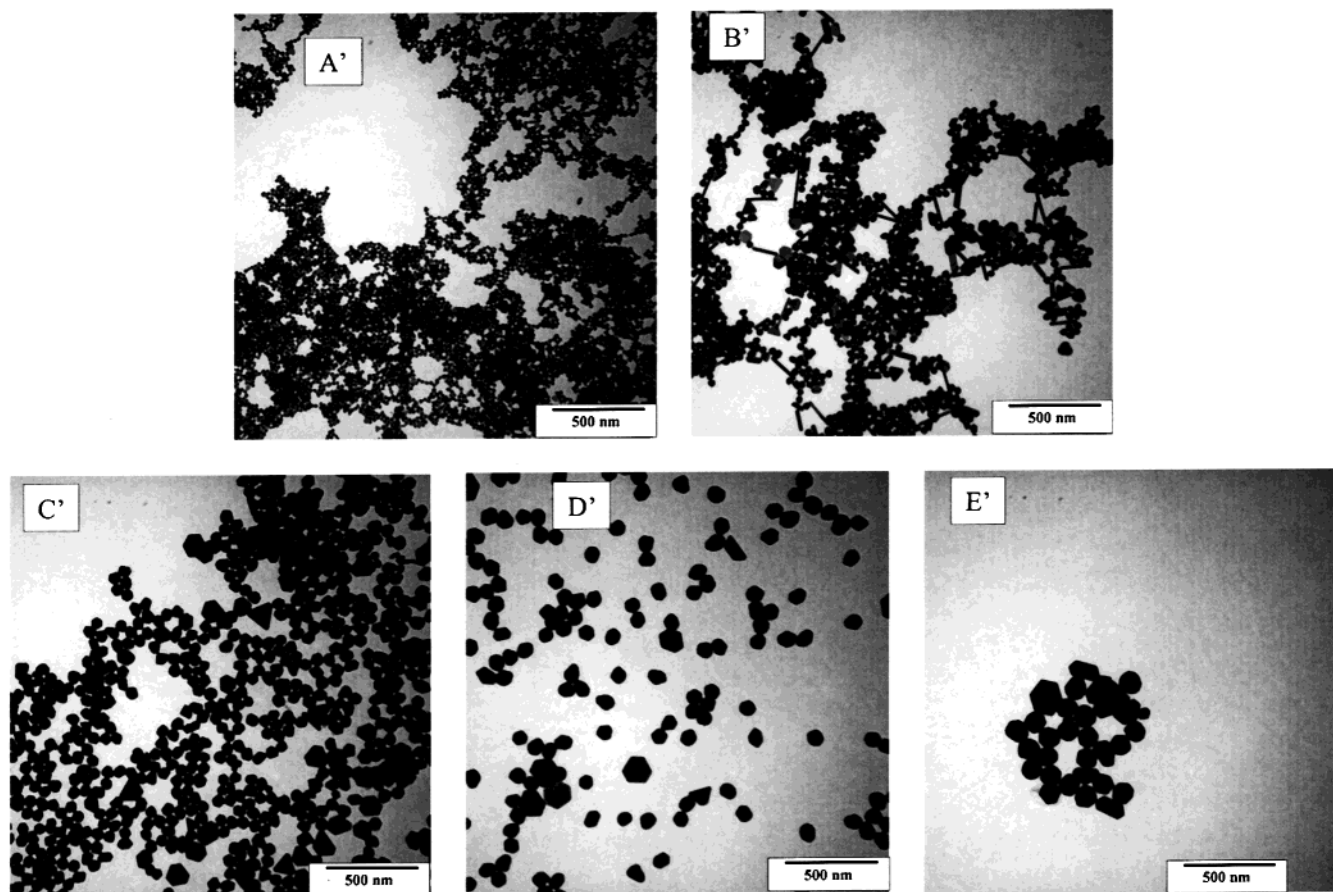


**Figure 5.** Representative electron micrographs of Au particles formed by slow addition of ascorbic acid corresponding to spectra A'–E' shown in Figure 4.



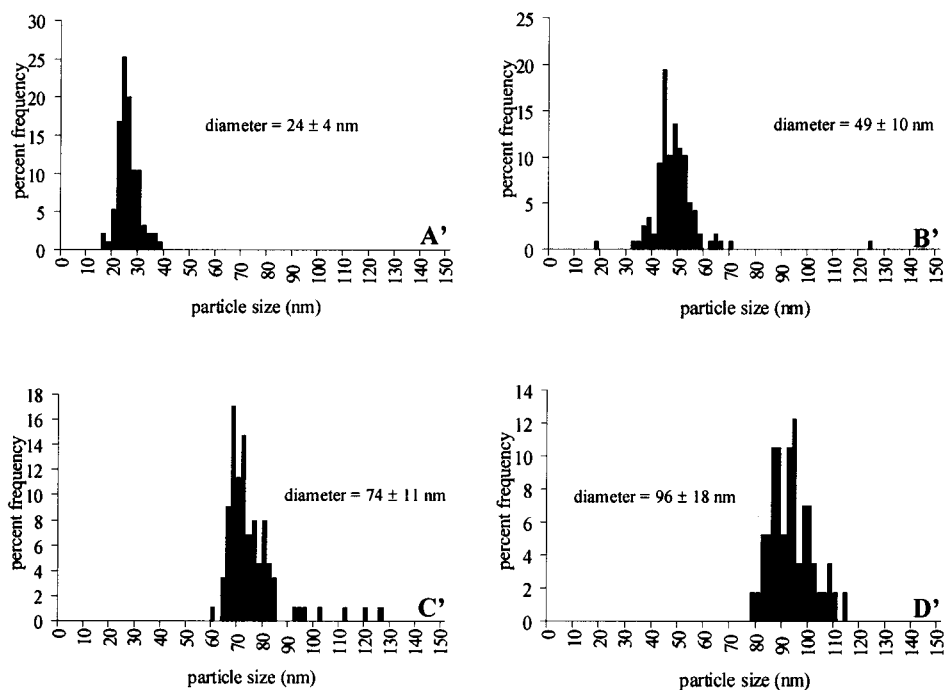


**Figure 6.** Size distribution histograms for Au particles (A'–D') formed by slow addition of ascorbic acid corresponding to Figure 5. The particles used for the size distribution in B' were prepared in the presence of  $\text{AgNO}_3$  to eliminate rod formation.

stabilizer for obtaining TEM images. For hydrazine reduction in the presence of 12 nm seed, most of the particles produced were 2–5 nm in diameter. In the absence of seed (but still with the addition of SDS), the gold nanoparticles were mostly 5–10 nm in diameter. Thus, seed-mediated nucleation events are also occurring with hydrazine as a reductant.

Sodium borohydride is a strong reducing agent that is capable of producing small gold nanoparticles at room temperature (diameter  $\sim 7$  nm) without the assistance of seeds. The presence of 12 nm gold seeds increases the average product particle size and widens the size distribution, indicating particle growth; thus, for this stronger reducing agent, there is little evidence for seed-mediated nucleation.

**Influence of the Ionic Conditions on the Formation of Gold Nanoparticles from Seeds.** During the course of the reaction,  $\text{HAuCl}_4$  is reduced to  $\text{Au}^0$ , with the concomitant release of chloride ions. It is possible that such free chloride ions could interact with gold species in solution and influence gold particle product formation. With the reaction conditions of method i, set D (fast addition of ascorbic acid, with a seed concentration that produced the greatest amount of particles smaller than seeds), we added additional NaCl (up to  $40 \mu\text{M}$ ) before the ascorbic acid or, alternatively, centrifuged the seed solution and redispersed the seeds in deionized water after removing supernatant in an attempt to remove loosely bound  $\text{Cl}^-$  from the seeds. In both cases, the gold particles formed were of the same average size as the original sample D.

In synthetic methods ii and iii, we noted the appearance of nonspherical gold particles. Other workers, in making gold nanorods electrochemically, have found that the presence of  $\text{AgNO}_3$  (with a rodlike surfactant) promotes rod formation over sphere formation, for reasons that are not clear.<sup>63</sup> Surprisingly, we observed that the addition of  $\text{AgNO}_3$  to our seeding growth

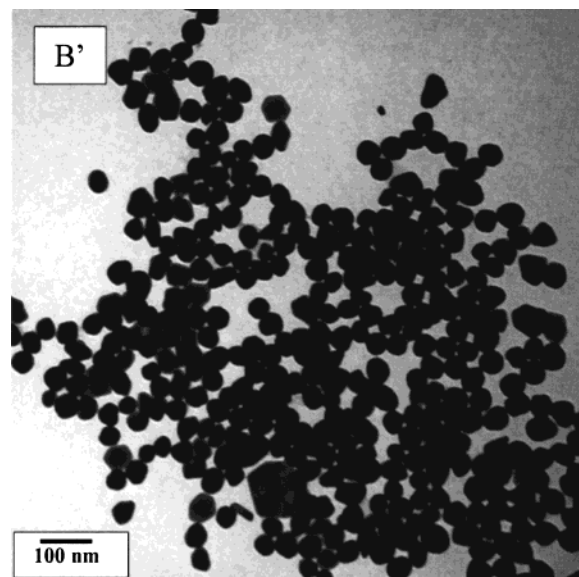


**Figure 7.** Electron micrograph of gold nanoparticles corresponding to set B' (Table 1) prepared in the presence of 20 mM  $\text{AgNO}_3$ . The presence of  $\text{AgNO}_3$  inhibits rod formation (compare to Figure 5B').

solutions without any rodlike surfactant eliminates the rodlike and platelet gold particles in methods ii and iii (Figure 7). The optimum silver ion concentration, we have found, is 1/50 of the total gold concentration to observe this effect. Metallic silver nanoparticles are not formed appreciably, on the basis of the absence of the  $\sim 400$  nm plasmon band of  $\sim 5$  nm or larger silver nanoparticles. We speculate that in the presence of halide counterions ( $\text{Cl}^-$  in our case,  $\text{Br}^-$  in the case of cetyltrimethylammonium bromide surfactant work<sup>63</sup>)  $\text{AgX}$  salts may form and serve as nucleation centers that

(63) Yu, Y. Y.; Chang, S. S.; Lee, C. L.; Wang, C. R. C. *J. Phys. Chem. B* **1997**, *101*, 6661.

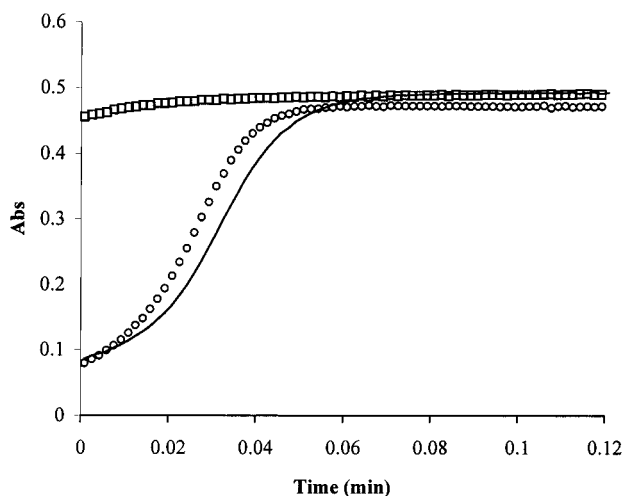


**Figure 8.** Kinetic plot of plasmon absorbance (at 530 nm) versus time: no seed (○); 1 mL of seed/mL of HAuCl<sub>4</sub> (—), set D; 50 mL of seed/mL of HAuCl<sub>4</sub> (□), set B. The final HAuCl<sub>4</sub> and SDS concentrations are 100 and 200 mM, respectively, for all samples.

complicate the kinetics of gold nanoparticle formation to favor spherical gold particles. This is consistent with the  $K_{sp}$  of AgCl in our case.

**Growth Kinetics.** The rate of gold nanoparticle growth in the presence of different amounts of seed was measured by monitoring the change in absorbance of the gold plasmon band at  $\sim 530$  nm as a function of time. We observed that the rates at which the solution changed color varied for different amounts of seed. Figure 8 shows the plot of absorbance vs time to be sigmoidal in the absence of seed. The sigmoidal shape of the plot is indicative of autocatalytic growth.<sup>26,37–42</sup> Figure 8 also shows the data for the same reaction but in the presence of different amounts of 12 nm seed; the synthetic conditions are those of method i for sets B and D (but in the presence of SDS to slow things down). For the larger amount of seed the plasmon band was at its maximum absorbance within the time of mixing; the rate on this time scale indicates that particle growth was very fast in the presence of a high amount of seed. However, in the presence of a small amount of seed, the growth rate and shape of the curve are similar to those observed without seed. It should be noted that gold nanoparticles of less than 1 nm have no plasmon band, and for 1–20 nm sized particles, the extinction coefficient at 525–530 nm increases with size.<sup>62</sup>

## Discussion

**Seed-Mediated Growth for Size Control.** There is a need to prepare monodisperse solutions of nanoparticles with well-defined dimensions. The seed-mediated growth method should offer the advantage of eliminating nucleation and promoting growth. In such cases, small metal particles are prepared and later used as seeds to prepare larger particles in the presence of a metal salt and a weak reducing agent.<sup>17d,44–53</sup> The concept of seeding growth to prepare monodisperse gold sols was developed by Zsigmondy et al.<sup>44</sup> and subsequently used by Turkevich et al.<sup>39</sup> Natan et al. reinvestigated the use of citrate- and borohydride-reduced gold particles as seeds for the preparation of larger Au

nanoparticles with diameters between 30 and 100 nm employing citrate or NH<sub>2</sub>OH as the growth stage reducing agent.<sup>17d,47</sup> They reported that the resulting larger particles exhibited improved monodispersity relative to those prepared in the one-step reduction of Au<sup>3+</sup> with citrate.<sup>17d</sup> Interestingly, repetitive seeding with NH<sub>2</sub>OH also led to the formation of a small percentage of cylindrical, high aspect ratio rods.<sup>17d</sup> Our work in this paper is consistent with Natan's.

Other metal nanoparticles have been prepared by seeding methods. Schneider et al. used borohydride-reduced 23 nm silver nanoparticle seeds to prepare larger silver particles.<sup>45,46</sup> Henglein et al. used  $\gamma$ -irradiated Cu, Ag, and Au seeds and CH<sub>2</sub>OH radical as a growth stage reducing agent for size control.<sup>48–50</sup> On the basis of a surface autocatalytic growth mechanism, Finke was able to prepare magic number Ir nanoclusters of different sizes (between 2 and 3 nm) using a seeded growth approach.<sup>53</sup>

In this work we have observed that the presence of seed can lead to nanoparticle products smaller than the seed, suggesting that seeds promote nucleation. This is a problem that other workers have observed.<sup>53–55</sup> However, controlling the rate of reagent addition directly influenced the product particle size and width of its distribution. Slow addition of a dilute solution of reducing agent suppressed additional nucleation, and we obtained larger particles with improved monodispersity in the size range of 20–100 nm (Tables 3 and 4). Additional nucleations can also be minimized by adjusting the ratio of seed to metal salt. For example, ascorbic acid-reduced gold nanoparticles prepared by fast addition generally showed a broad size distribution ( $22 \pm 10$  nm, Figure 3F) when no seed was present; the presence of seed can improve monodispersity when growth predominates over nucleation (set A, Figure 3A,  $20 \pm 6$  nm). The size distributions we obtained are all similar to those achieved by the Natan group, who employed a similar seed-mediated growth method.<sup>17d</sup>

To make particles 1–10 nm in size by seed-mediated growth requires the use of a smaller seed. We have prepared borohydride-reduced 3–4 nm gold nanoparticles in the presence of citrate (the citrate in this case served as a capping agent). By using 3–4 nm sized gold particles as seeds, we can make particles 5–30 nm in size in an aqueous surfactant medium (data not shown).

Another common problem in preparing larger spherical particles by seeding growth is the generation of faceted or rodlike particles. In reduction without seeds, these faceted particles are occasionally observed for weak reducing agents where growth occurs over a longer period.<sup>25</sup> El-Sayed et al. provide two reasonable explanations for the formation of faceted and rod-shaped particles: (i) the growth rates vary at different planes of the particles and (ii) particle growth competes with the capping action of stabilizers (in our case ionic reagents).<sup>64</sup> When  $\sim 50$  nm particles were prepared from the same size seed, the particle shapes were more spherical (Figure 2B) for faster addition of reducing agent but faceted (as well as rod and platelet shaped) (Figure 5B') for slow addition of reducing agent. Sets B'–E' prepared by slow addition of reducing agent all

(64) Petroski, J. M.; Wang, Z. L.; Green, T. C.; El-Sayed, M. A. J. *Phys. Chem. B* **1998**, *102*, 3316.



contain faceted and rodlike particles (Figure 5). But for faster addition, only E and F contained rods and facets (Figure 2), where either no seed or a relatively small amount of seed was used. This is consistent with earlier works.<sup>25</sup> We found in related works that the addition of a rodlike micellar template in seed-mediated growth increases the rod yield.<sup>65</sup>

The success of earlier seed-mediated growth approaches is due to enhanced autocatalytic growth over additional nucleation.<sup>17d,44–53</sup> The seeds can act as nucleation centers and grow due to the reduction of bulk metal ions at their surfaces. The reducing agent is chosen so that metal ion reduction takes place only at the surface of the seed particle without generating any additional nucleation centers; thus, particle sizes are controlled by varying the ratio of seeds to metal ions.

A widely used means of controlling particle size is to employ a capping agent. The stabilizer that strongly caps the particles inhibits the growth, thus generating high monodispersity. There are examples indicating capped metal particles act as electron-transfer catalysts<sup>66</sup> as well as initial nucleation centers for inorganic crystals.<sup>67</sup> Therefore, one reason for the higher monodispersity of direct citrate-reduced gold nanoparticles may be due not only to the good capping action of citrate,<sup>49</sup> but also to the active redox catalytic properties of citrate-capped gold particles. A similar mechanism may also contribute to thiol-capped metal nanoparticles for high monodispersity.

Thus, seed-mediated growth can be used for gold nanoparticle size control. The size can be controlled by varying the ratio of seed to metal salt. The additional nucleations beyond seed can be minimized by slowly adding the reagents. But the slow addition rate often causes shapes other than spheres, particularly for making larger sized particles.

**Seed-Mediated Nucleation: Another Mechanistic Step To Consider.** The observation of seeds promoting nucleation in our experiments assists in explaining the particle formation mechanism in chemical reduction of metal salts. The particle size distribution depends on the interplay between the nucleation and growth that occurs at the intermediate stage. Because of the size-dependent redox property of metal clusters, the redox potential of  $M_{\text{atom}}/M_{\text{ion}}$  is very negative, and thus initial reduction (hence the nucleation) of salt by a reducing agent is either slow or absent. In our case, the reduction potential for the  $\text{Au}_{\text{metal}}/\text{Au}^{\text{I}}$  (aqueous) system is +1.68 V versus NHE, according to *Lange's Handbook of Chemistry*, but for a  $\text{Au}_{\text{atom}}/\text{Au}^{\text{I}}$  (aqueous) system, it is -1.5 V versus NHE.<sup>29,32</sup> Ascorbic acid, being a weak reducing agent (reduction potential +0.125 V vs NHE), cannot reduce gold salt; therefore, preformed metallic seed must catalyze the reduction processes. Such catalytic reduction is due to particle-mediated electron transfer from ascorbic acid to gold ions. However, reduction rates differ depending on the addition rate of ascorbic acid, thus influencing the particle size and size distribution. For slow addition

rates, only growth is observed, but for faster addition rates, both nucleation and growth occur. Another important observation of our seed-mediated reduction is that the extent of additional nucleation varies depending on the ratio of seed to metal salt, and a smaller number of seeds can lead to a burst of nucleation (Table 3).

In the absence of preformed seed, ascorbate reduction of gold salt could be slowly catalyzed by the surface of the reaction vessel, and thus we observe an induction period or purple film of gold when ascorbic acid is slowly added. A similar promoting effect of the reaction vessel or foreign solids (silica particles) was observed for alcohol reduction of gold salt.<sup>37</sup> During the induction period, some nucleations are slowly formed and can be considered as seeds. The appearance of these nucleations, or seeds, catalyzes the reduction processes similar to our seed-mediated reduction in methods i and ii. Thus, in the next stage, seed-mediated nucleation and growth occur simultaneously, and the number of particles rapidly increases as the reaction progresses. After a critical particle concentration is reached (similar to our samples C–E), a nucleation burst occurs. The only difference with respect to seeding reduction may be the time and extent of additional nucleation. After the nucleation burst, the ratio of particle to metal ion is increased, and growth predominates over nucleations, as was observed in our seeding reduction.

Gaining complete understanding of the mechanism requires the capabilities to measure relative sizes and concentrations of the particles at any point throughout the reaction. Unfortunately, even high-resolution electron microscopy cannot reveal initial nucleation, and sample preparation for electron microscopy can lead to aggregation, thus complicating interpretations of the results. Despite the experimental difficulty in studying intermediate stages of particle formation, several attempts have been reported which support our proposed nucleation burst. Rao et al. estimated the time evolution of particle size distribution for gold particles and found that both the average size and standard deviation increase with time.<sup>56</sup> Similar results were observed for citrate-reduced gold.<sup>57</sup> Another point to consider is the possibility that the 12 nm seeds might contain additional gold nanoparticles too small to visualize by TEM, and that these "invisible" nanoparticles grow. Indeed, for gold nanoparticles supported on carbon, there are X-ray diffraction data to suggest that this might be the case under certain conditions.<sup>68</sup> We have observed ~2 nm Au nanoparticles in syntheses in which we make ~3 nm seeds, but have not observed these in the present 12 nm seed case; also, this "invisible seed" idea does not explain why fast addition of reducing agent would cause these sub 2 nm seeds to grow, but slow addition of reducing agent does not. Also, the calculated diameters of nanoparticles assuming only growth are close to the observed experimental values for all slow addition conditions (Table 4) and sets A and B for fast addition (Table 3). Nonetheless, we performed several experiments to examine this alternate hypothesis. We attempted to size-selectively extract any sub 2 nm nanoparticles from the 12 nm seeds with various

(65) Jana, N. R.; Gearheart, L.; Murphy, C. J. *Adv. Mater.*, for publication.

(66) Ung, T.; Liz-Marzan, L. M.; Mulvaney, P. *J. Phys. Chem. B* **1999**, *103*, 6770.

(67) Küther, J.; Sehadi, R.; Nelles, G.; Assenmacher, W.; Butt, H.-J.; Mader, W.; Tremel, W. *Chem. Mater.* **1999**, *11*, 1317.

(68) Riello P.; Canton, P.; Benedetti, A. *Langmuir* **1998**, *14*, 6617.

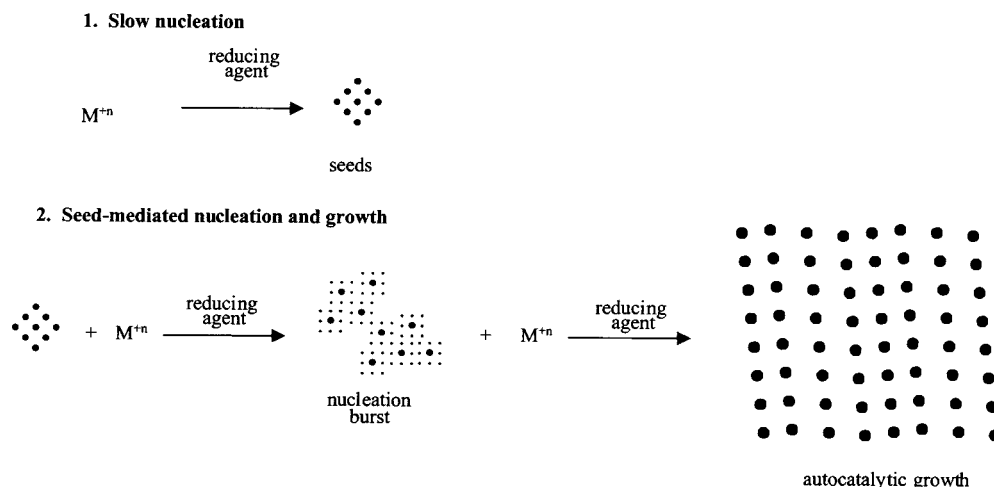


**Figure 9.** Generalized two-step mechanism for solution-phase Au nanoparticle synthesis.

centrifugation/precipitation schemes, and reran the growth steps with each fraction. In all cases the 12 nm seeds behaved as they had before, while the “sub 2 nm seed” fractions behaved as the no-seed case. We also attempted X-ray powder diffraction experiments of the 12 nm seeds as per ref 68, but the broadening of the Au powder-pattern lines did not require the supposition of an additional substantial population of sub 2 nm nanoparticles to explain the data. Thus, at present, we have no data that prove that sub 2 nm Au seeds exist in the 12 nm Au seed solutions at significant concentrations.

Literature regarding nanoparticle synthesis commonly includes the final size distribution of particles as opposed to intermediate sizes. Often the size distributions are actually quite sharp, even for weak reducing agents that, according to the size-dependent redox property of metal clusters, should not reduce the metal salts. Examples include citrate- and formamide-reduced gold sols, ascorbate-reduced gold and silver sols, alcohol-reduced gold sols, etc.<sup>25,39,40,42</sup> For these weak reducing agent systems, reduction depends on a critical condition of the appearance of seeds (nucleation centers). Those seeds will grow larger and larger, as metal ion reduction is possible only at the seed surface. From this analogy, only heavily developed micrometer sized particles are expected; in actuality, a range of nanosized particles form. Matijevic et al. prepared micrometer sized gold particles that are aggregates of nanosized precursors. For this they used ascorbic acid reduction of gold salt.<sup>59</sup> They proposed a nucleation burst at an intermediate stage to form nanosized precursors that subsequently aggregate to form microparticles.

From our observed results, we propose a mechanistic step in gold nanoparticle formation that incorporates seed-mediated nucleation. From kinetic evidence Finke et al. proposed continuous slow nucleation with fast autocatalytic growth for transition-metal nanocluster formation.<sup>26</sup> This proposed mechanism can explain the observed narrow size distribution due to the separation

of nucleation and growth in time.<sup>26</sup> Our results for gold nanoparticle synthesis suggest that nucleation is a slow process at the beginning of the reaction, followed by simultaneous nucleation and growth mediated by the early nucleations. Thus, nucleation rapidly increases as the reaction progresses, then slows down, and eventually stops (so the particle concentration becomes constant) as growth predominates. Accordingly, we propose a two-step mechanism: an initial slow nucleation, followed by a burst of nucleation mediated by seeds and growth (Figure 9).

## Conclusion

We studied seed-mediated reduction of gold salt by ascorbic acid using 12 nm gold seeds. We observed that particle size can be controlled by varying the seed to metal salt. However, for lower seed to metal salt ratios, additional nucleation events widen the size distribution. Slower addition of reducing agent inhibits additional nucleations but promotes nonspherical products.

New insights about the mechanism of nanoparticle synthesis are gained from this study. In particular, we propose a seed-mediated nucleation step that could fruitfully be examined and perhaps exploited in metallic nanoparticle syntheses.

**Acknowledgment.** We thank the National Science Foundation for funding and the anonymous reviewers for critical comments. We also thank Professor H. zur Loye and his group for assistance with the powder diffraction experiments.

**Supporting Information Available:** Transmission electron micrographs of Au nanoparticles prepared with different reducing agents in the presence and absence of seed (PDF). This material is available free of charge via the Internet at <http://pubs.acs.org>.

CM000662N